Progress In Electromagnetics Research C, Vol. 106, 17–27, 2020

A Circuit-Coupled FEM Model with Considering Parasitic Capacitances Effect for Galvanic Coupling Intrabody Communication

Zhiying Chen[1, *], Yueming Gao[2, 3], Min Du[3, 4], and Feng Lin[2, 3]

Abstract—Characterization of the human body channel is a necessity to pave way for practical implementation of intrabody communication (IBC) in body area networks (BAN). In this paper, a circuit-coupled finite element method (FEM) based model is proposed to represent the galvanic coupling type IBC on human arm. In contrast with other models for IBC, both the finite element method and the parasitic capacitances between electrodes are taken into account in the modeling. To understand the characteristics of IBC, simulations with multiple frequencies, excitation voltages, channel lengths and values of parasitic capacitors are carried out using the model. The current density and electric field distribution in different human tissues reveal an insight into signal transmission path through the human body intuitively. The body channel gain presents a band-pass property after adding the parasitic capacitances into the model, while it performs an increasing characteristic with the frequency before the adding. Finally, a galvanic coupling IBC measurement setup is fulfilled, and the outcome shows a good agreement with the proposed model. It is indicated that the parasitic capacitances are the major factors to cause the band-pass and affect the bandwidth, and they should not be neglected in the real IBC applications.

1. INTRODUCTION

Intrabody communication (IBC) is an emerging wireless communication technology which uses human body as a signal transmission channel [1]. The concept of this technique is to employ near field or electrostatic coupling instead of electromagnetic wave between the transmitter and receiver. It helps to reduce the power consumption, minimize the volume, and enhance the communication security of the electronic devices [2]. It has been defined as an important connecting technique for BANs in the IEEE 802.15.6 protocol [3]. Thus, it will be extensively used in the healthcare and clinical application, such as wearable electric health monitoring devices.

There are two basic methods of signal coupling between transmitter and receiver in IBC system: capacitive coupling and galvanic coupling [4]. In the former, the transmission quality is easily affected by the noisy environment and the size of the receiver ground planes, and the signal return path from the transmitter to the receiver ground electrodes is closed through the environment [5]. In the latter, which is the focus of this study, the signal current flows through the human body as it is transmitted from a pair of transmitter electrodes to a pair of receiver electrodes. Accordingly, the transmission quality is not affected easily by the surroundings of human body, especially in low frequency communication. In order to know the galvanic coupling IBC behavior better, it is significant to investigate the transmission properties of human body channel.

Received 27 July 2020, Accepted 15 September 2020, Scheduled 5 October 2020

* Corresponding author: Zhiying Chen (chzy207@163.com).

[1] School of Electrical Engineering & Automation, Xiamen University of Technology, Xiamen, Fujian 361024, China. [2] Key Laboratory of Medical Instrumentation & Pharmaceutical Technology of Fujian Province, Fuzhou University, Fuzhou, Fujian 350116, China. [3] College of Physics and Telecommunication Engineering, Fuzhou University, Fuzhou, Fujian 350116, China. [4] Fujian Provincial Key Laboratory of Eco-Industrial Green Technology, Wuyi University, Wuyishan, Fujian 354300, China.

Several groups have dedicated to the research of propagation mechanism in galvanic coupling IBC. There are many different calculation methods having been proposed for IBC modeling, such as finite element method (FEM) [6, 7], quasi-static field theory model [8], equivalent electrical circuit model [9–13], and Field-Circuit FEM [14, 15]. Among them, FEM and circuit model has been most widely used in IBC. However, after implementing the FEM model, circuit model, and experiment on forearm with the frequency from 1 kHz to 1 MHz, we have found that there is a big contradiction between the models and experiment. The results of our measurement revealed that the human body channel performed as a band-pass characteristic, whereas except [12] and [13], the receiver voltage gains of the FEM and circuit models [6–11] were presented as an increase with the frequency. Due to the smaller frequency range from 100 kHz to 1 MHz studied in [12, 13], the gain primarily showed a decline not a band-pass with frequency. The main reason for the contradiction is supposed as that most of the IBC models only used one of the methods mentioned above and rarely adopted multiple approaches together for modeling. Generally, FEM is often used to calculate the electric and current field distribution of the IBC model which can be described as a group of second order partial differential equations (PDEs), but the electrical effects between electrodes to the transmission are usually neglected. Thus, the parasitic capacitances between electrodes are unable to be computed together with the FEM model, and it will lead to a big dissimilitude of model results relative to the experiment results eventually. In that case, a circuit-coupled FEM was proposed to provide useful insights into the capacitive coupled IBC in [14], where the parasitic return path between the electrode and ground was simplified by an equivalent capacitor. Next, a field-circuit FEM model was presented in [15] to estimate the channel gain for galvanic coupling IBC, where the parasitic impedance between electrodes was first taken into account in modeling. However, because of the approximate zero conductivity of the air, the effect between electrodes should be equivalent to the parasitic capacitance rather than the impedance. Therefore, the model in [15] has an obvious defect and should be improved.

In this study, we propose a new modeling method for the galvanic coupling signal transmission of the human arm based on a circuit-coupled FEM model in which the parasitic capacitances between electrodes are considered. With the help of COMSOL MULTIPHYSICS, the transmission characteristics of human body tissues are simulated by using finite element method, and the effects of parasitic capacitances between electrodes are simulated with simplified circuits. Compared with other methods presented in [6–15], more affecting factors and parameters of IBC are taken into account in our modeling, such as interelectrode effects (parasitic capacitance), electrode own influences, much wider frequency (a lot of studies only investigate the frequency from 10 kHz to 1 MHz), and different applied voltages. By carrying out a galvanic coupling IBC experiment on a human arm, the proposed model is also found to match the measurement much better than others. To the best knowledge of the authors, this is the first report on taking parasitic capacitances into account for galvanic coupling IBC modeling.

2. CIRCUIT-COUPLED FEM MODEL

2.1. Model Definition

The geometry considered in this study consists of a multilayered cylinder modeling a human arm formed by five different concentric layers, each of which simulates a different tissue: skin, fat, muscle, cortical bone, and cancellous bone. The detailed illustration is shown in Fig. 1, and the main geometry parameters are listed in Table 1, respectively. The tissue thicknesses are within the range of true anatomical proportions and refer to those proposed in [7]. The frequency behavior of dielectric properties of tissues, such as conductivity and permittivity, is derived from the parametric modes of Gabriel et al. [16] who summarized measurements from *in vivo* experiments on the human body and autopsies of cadavers and animals. An outer layer has also been considered in order to simulate an unbounded and grounded air domain surrounding the human arm. By doing so, deviations are able to be reduced to the minimum.

Finally, two pairs of 4 cm $*$ 4 cm squared copper electrodes are placed on the skin at the determined distance l_e, l_s. The electrodes are connected to the external circuit as shown in Fig. 2. Resistances R1, R2, R3, R4 and capacitors C1, C2, C3, C4 are the simplified equivalent circuit model of the real medical electrodes LT-1 used in IBC measurement. LT-1 was found to have both resistive and capacitive properties by test, so a resistance and a capacitor are in parallel to simulate the effects. R1, C1, and

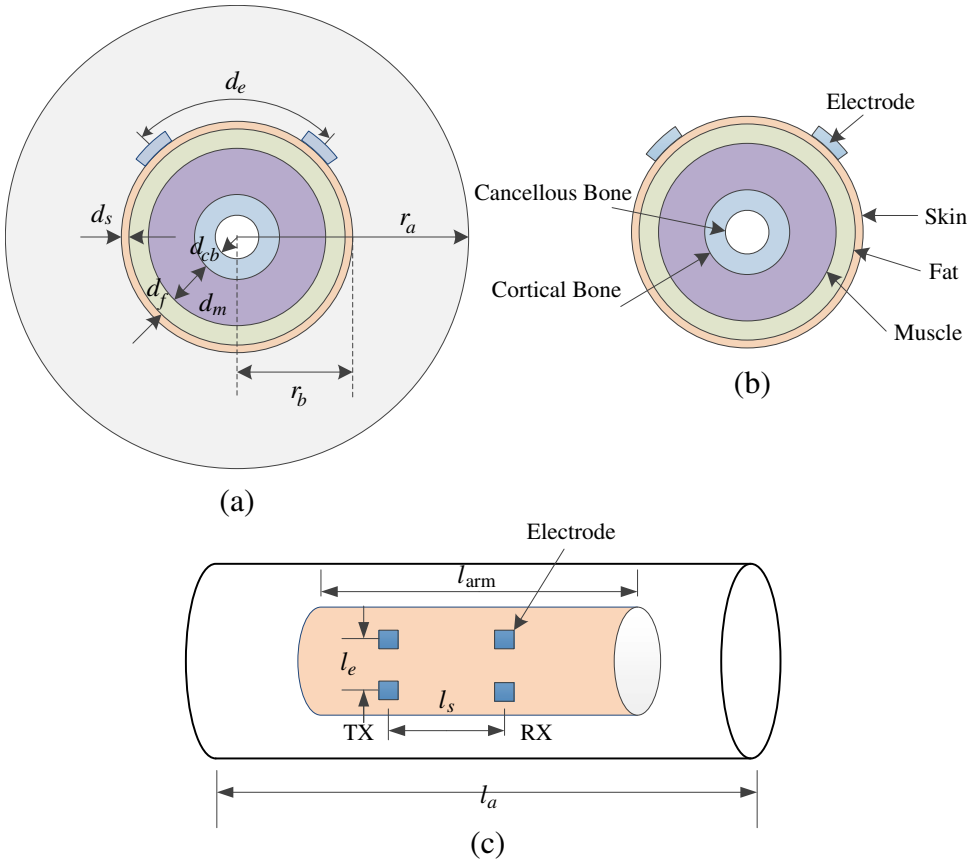

Figure 1. Geometry of the proposed model. (a) Transverse section of the arm inside an external air layer. (b) Transverse section of the arm composed of five concentric layers of tissues: skin, fat, muscle, and cortical and cancellous bone. (c) Longitudinal view of the arm with electrodes, depicting parameters such as channel length (l_s), inter-electrode distance (l_e), arm length (l_{arm}), etc.

Table 1. Geometry parameters of galvanic coupling model.

Parameter	Value	Description
r_a	10 [cm]	External air layer radius
l_a	120 [cm]	External air layer length
r_b	5 [cm]	Arm radius
l_{arm}	60 [cm]	Arm length
d_s	1.5 [mm]	Skin thickness
d_f	8.5 [mm]	Fat thickness
d_m	27.5 [mm]	Muscle thickness
d_{cb}	6 [mm]	Cortical Bone thickness
l_e	8 [cm]	Inter-electrode distance
l_s	5, 10, 15 [cm]	Signal channel length

R3, C3 are respectively used to simulate the positive and negative TX electrodes. Similarly, R2, C2 and R4, C4 are respectively used to simulate the two RX electrodes. These RC modules are deemed to be in series with TX or RX terminals due to the attachment of LT-1 on skin. There are parasitic capacitance effects between any two electrodes, thus capacitors C5, C6, C7, C8 are used to simulate

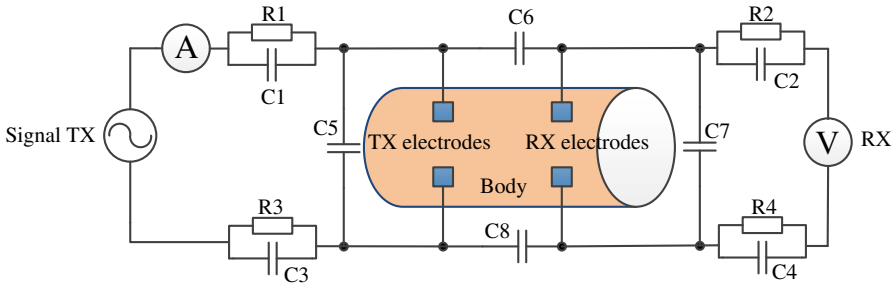

Figure 2. Schematic of model connected to the external circuit with signal source and impedance.

these effects and are in parallel with their respective electrodes. C5 represents the parasitic capacitance between the TX electrodes. C7 represents the parasitic capacitance between the RX electrodes. C6 and C8 represent the parasitic capacitances between TX electrodes and RX electrodes. The values of these circuit parameters are referred to [17] in which equivalent electric parameters of electrodes are proposed to be measured by LCR meter. In addition, an AC voltage source is applied on the transmitter side to generate signal, and a voltage meter is placed on the receiver side to acquire the electric potential difference.

2.2. Model Equations and Simulation Setting

In terms of Maxwell equations, the electromagnetic field can be simplified as a quasi-static field when the wavelength λ or skin depth δ is much larger than the dimensions of studied domain. Table 2 lists the verification of the quasi-static criteria about human body tissues. It is clear to find that the wave propagation effects can be negligible definitely because most ratios between the tissue thickness and

Table 2. Verification of the quasi-static criteria.

	Frequency (Hz)	Conductivity σ (S/m)	Relative permittivity ε_r	Wave length λ (m)	Capacitance effect	Propagation coefficient k
Bone (cortical)	1k	2.00e − 02	2.70e + 03	7.04e + 02	7.50e − 03	8.92e − 03
	100k	2.10e − 02	2.30e + 02	6.69e + 01	6.08e − 02	9.39e − 02
	1M	2.40e − 02	1.40e + 02	1.74e + 01	3.24e − 01	3.61e − 01
	10M	4.30e − 02	3.68e + 01	3.83	4.75e − 01	1.64
	100M	6.43e − 02	1.53e + 01	7.22e − 01	1.32	8.70
Muscle (across)	1k	3.20e − 01	4.30e + 05	1.70e + 02	7.47e − 02	3.69e − 02
	100k	3.60e − 01	8.10e + 03	1.57e + 01	1.25e − 01	4.01e − 01
	1M	5.00e − 01	1.80e + 03	4.05	2.00e − 01	1.55
	10M	6.17e − 01	1.71e + 02	1.14	1.44e − 01	5.49
	100M	7.08e − 01	6.60e + 01	2.93e − 01	5.18e − 01	2.14e + 01
Fat	1k	2.24e − 02	2.41e + 04	6.48e + 02	5.98e − 02	9.69e − 03
	100k	2.44e − 02	9.29e + 01	6.33e + 01	2.12e − 02	9.92e − 02
	1M	2.51e − 02	2.72e + 01	1.94e + 01	6.02e − 02	3.24e − 01
	10M	2.92e − 02	1.38e + 01	5.14	2.63e − 01	1.22
	100M	3.63e − 02	6.07	1.10	9.29e − 01	5.73
Wet skin	1k	6.60e − 04	3.20e + 04	1.65e + 03	2.72	3.81e − 03
	100k	6.60e − 02	1.50e + 04	2.28e + 01	1.30	2.74e − 01
	1M	2.20e − 01	1.80e + 03	5.38	4.60e − 01	1.16
	10M	3.66e − 01	2.22e + 02	1.40	3.37e − 01	4.49
	100M	5.23e − 01	6.60e + 01	3.15e − 01	7.00e − 01	1.99e + 01

wavelength lambda in different tissues are less than 0.1 when the frequency is lower than 10 MHz [18], for most ratios of arm length l_{arm} to wavelength λ in different tissues are less than 0.1 with the frequency. Then the proposed model is implemented in COMSOL MULTIPHYSICS 5.0 by using the Electrical Circuit interface and Electric Current interface within the AC/DC module. Electrical Circuit interface, which solves Kirchhoff's conservation laws for the voltages, currents, and charges associated with the circuit elements, is used to simulate the effect of electrodes to the human arm transmission. Electric Current interface, which solves a current conservation equation based on differential Ohm's law, is used to compute electric field, current, and potential distributions in human arm which is regarded as a quasi-static electric field. Frequency domain study is selected, and the corresponding solving equations are as follows:

$$\mathbf{J} = \sigma\mathbf{E} + j\omega\mathbf{D} + \mathbf{J}_e \tag{1}$$

$$\nabla \cdot \mathbf{J} = Q_j \tag{2}$$

$$\mathbf{E} = -\nabla V \tag{3}$$

$$\mathbf{D} = \varepsilon_r\varepsilon_0\mathbf{E} \tag{4}$$

where $\mathbf{J}$ is the current density [A/m^2], σ the electrical conductivity [S/m], $\mathbf{E}$ the electric field intensity [V/m], J_e the source current density [A/m^2], ω the angular frequency [rad/s], V the scalar electric potential [V], Q_j the boundary current source [A/m^2], D the electric displacement [C/m^2], ε_r the relative permittivity, and ε_0 the permittivity of vacuum [F/m].

In Electric Current interface setting, the whole study domain is chosen for the Current Conservation node firstly; then the outer air layer is chosen for the Electric Insulation node; the air domain is set as an infinite element domain which is used for the simulation of unbounded or infinite domains; and finally, Terminal nodes is chosen for the four electrodes to provide a boundary condition for the connection to external circuits. The signal excitation to arm model is added in the external circuit by an AC voltage source whose amplitude and frequency vary from 0.5 V to 3 V and from 100 Hz to 10 MHz. Four External I-Terminal nodes are added in Electric Circuit interface setting to realize the connection with Terminal nodes in electric curren interface. Then, a fine free tetrahedral element is used to mesh the arm geometry, and a swept meshing technique is used to mesh the external air layer. After meshing, the solving for the model is run by using the direct solver PARDISO in the fully coupled way. In addition, in order to compute the model in a loop automatically with different frequencies and voltages, a parameter sweep mode is set in the solver configurations. The detailed parameters of model solving are listed in Table 3.

Table 3. Simulation parameters of model.

Amplitude of excited voltage (V)	0.5, 1, 1.5, 2, 2.5, 3
Frequency of excited voltage (Hz)	100, 200, 300, 400, 500, 600, 700, 800, 900, 1e3, 2e3, 3e3, 4e3, 5e3, 6e3, 7e3, 8e3, 9e3, 1e4, 2e4, 3e4, 4e4, 5e4, 6e4, 7e4, 8e4, 9e4, 1e5, 2e5, 3e5, 4e5, 5e5, 6e5, 7e5, 8e5, 9e5, 1e6, 2e6, 3e6, 4e6, 5e6, 6e6, 7e6, 8e6, 9e6, 1e7
Channel length (cm)	5, 10, 15

2.3. Simulation Results

The distributions of electric current density in different human body tissues are concerned about firstly. With the help of the strong post-processing ability in COMSOL MULTIPHYSICS, the relevant physical quantities of electric field are easy to be observed by 3D, 2D, or 1D plot. Accordingly, two groups of cross-sectional planes plots about current density with different frequencies at the transmitted voltage

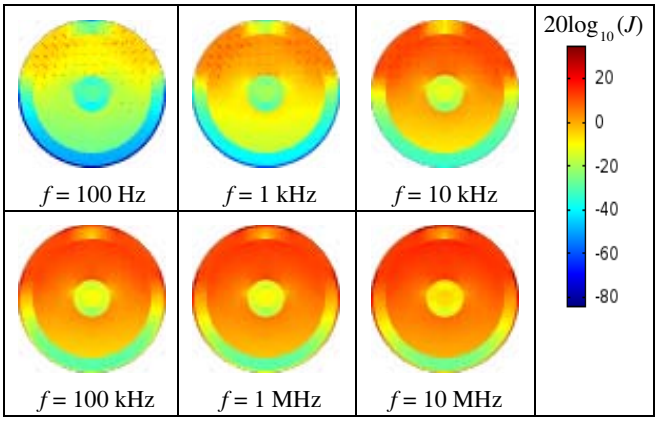

(a)

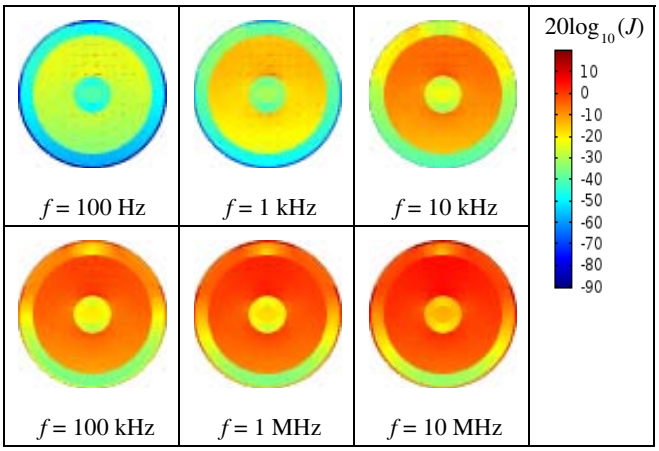

(b)

Figure 3. Distribution of current density in body tissues. (a) Current density of the section across transmitter. (b) Current density of the section across receiver.

3 V are drawn, as shown in Fig. 3. One group of sections is across the transmitter, and the other is across the receiver. The figure shows that the current density J in all tissues increases with the frequency increment. Moreover, J is the largest in muscle and smallest in skin when the frequency is lower than 100 kHz, which means that the current primarily flows over the muscle. However, when the frequency is higher than 100 kHz, the current density J in skin increases with the frequency greatly and even much larger than that in muscle, which means that the skin effect is more obvious with frequency increment. It should also be noticed that the current density J in the bone is always small at all frequencies.

Subsequently, the distribution of the electric field is analyzed in different tissues at the same transmitted voltage of 3 V, as shown in Fig. 4. The electric field strength E is very large in the skin near the transmitter electrodes while E in other areas is very small at the frequency of 100 Hz, which means that E primarily exists in the skin. However, with the frequency increment, E in all domain except for the skin near the transmitter electrodes increases gradually with frequency. We notice that these varieties of electric field E and current density J are according to the Ohm's law $J = \sigma E$. In order to show the comparison between results at different frequencies clearly with the same color range, logarithmic computation $20\log_{10}(J)$ and $20\log_{10}(E)$ are used to describe the current density J and electric field E in Fig. 3 and Fig. 4.

Finally, the most significant parameter, the ratio between received voltage and transmitted voltage is calculated to find the difference between circuit-coupled FEM model and FEM model. A solution is also solved with the FEM model whose external circuit is removed. The received voltages of two models

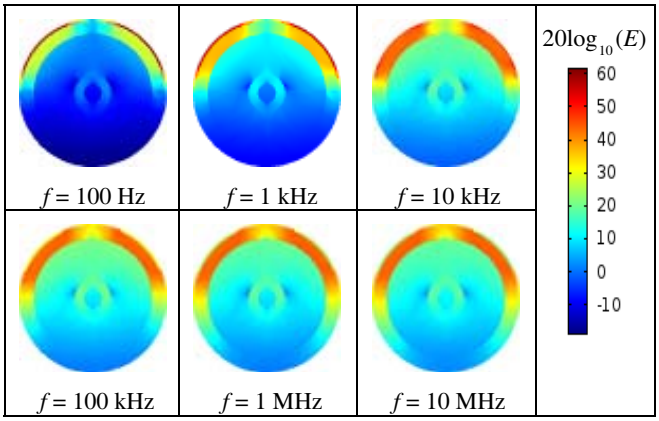

(a)

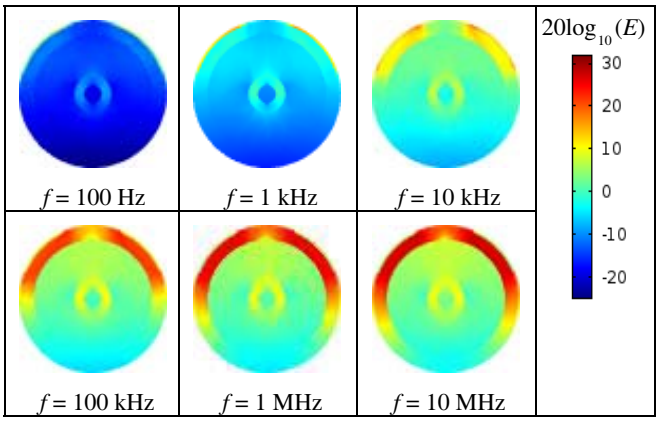

(b)

Figure 4. Distribution of electric field in body tissues. (a) Electric field of the section across transmitter. (b) Electric field of the section across receiver.

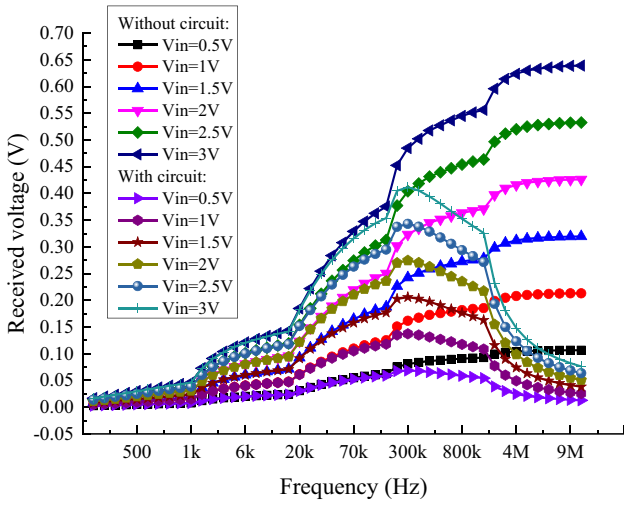

Figure 5. Received voltage of two models.

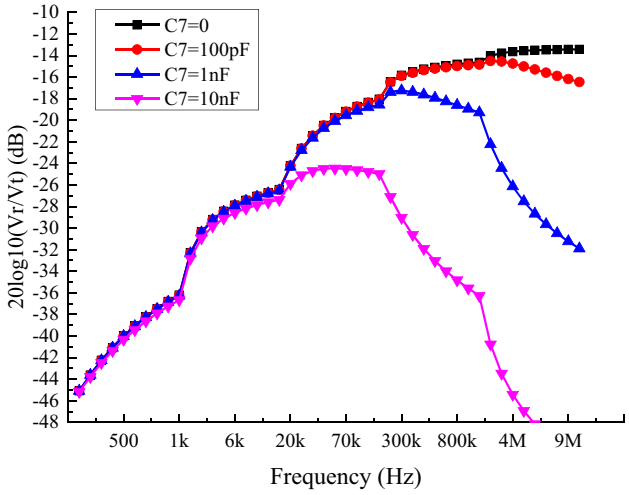

Figure 6. Voltage gain of model with different parasitic capacitance C7 between received electrodes.

and the comparison between them are shown in Fig. 5. The received voltages in FEM model always increase with frequency; however, those in circuit-coupled FEM model have the same values about below 300 kHz while decreases above 300 kHz. Consequently, it is supposed that the signal attenuation of human body channel with frequency is mainly caused by the parasitic capacitances between external transmitted or received electrodes. The parasitic capacitances (especially between received electrodes) affect the passband of signal channel greatly. Fig. 6 shows the gain of voltage signal with different values of the equivalent parasitic capacitance C7 between received electrodes. The cut-off frequency of signal is inversely proportional to the value of C7, which means that the passband is narrow when C7 is large.

3. MEASUREMENT SETUP

In order to validate the model, a galvanic coupling IBC measurement on human arm is carried out. The measurement setup consists of a signal generator and a balun at the transmitter side (TX), a digital oscilloscope at the receiver side (RX), and four 4 cm ∗ 4 cm medical electrodes LT-1 attached to the skin in a differential configuration [19], as shown in Fig. 7. It should be noticed that a differential probe must be used to test the received signal so that the electromagnetic interference from AC source can be eliminated. However, the balun and differential probe can be removed when the oscilloscope uses the battery supply. The excited signal between the two transmitter electrodes adopts a sine voltage of whom the peak-to-peak value changes from 1 V to 6 V, and the frequency changes from 100 Hz to 10 MHz. In addition, with the aim of analyzing the effect of channel length to the transmission quality, different channel lengths l_s from 5 cm to 15 cm are tested. All the relative testing parameters are the same as those in Table 3.

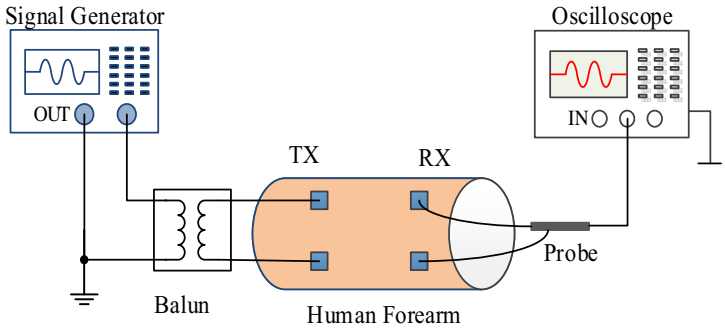

(a)

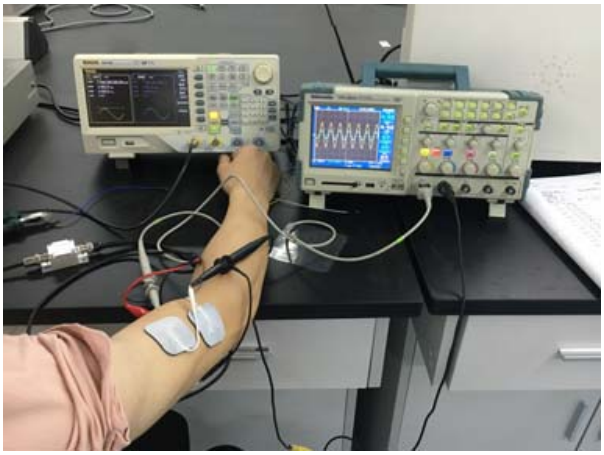

(b)

Figure 7. Galvanic coupling measurement setup. (a) Measurement circuit. (b) Measurement scene.

4. RESULTS AND DISCUSSIONS

Figures 8 and 9 show the received voltage and gain of galvanic coupling IBC experiment on a 23-year-old male volunteer. The two figures obviously indicate that the property of body channel performs as a band-pass characteristic. Compared with the simulation results (shown in Fig. 5 and Fig. 6), the circuit-coupled FEM model is more suitable for voltage-excited galvanic coupling IBC modeling, and the attenuation of received signal with frequency is primarily caused by the parasitic capacitances between received electrodes.

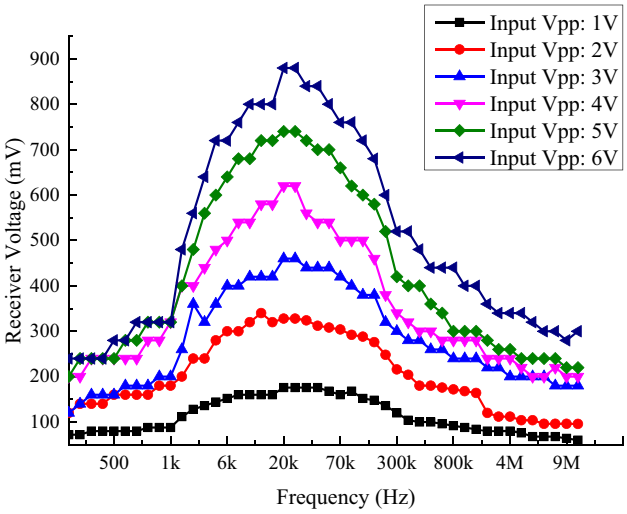

Figure 8. Received voltage of arm IBC measurement. The value corresponding to a signal channel length of 5 cm.

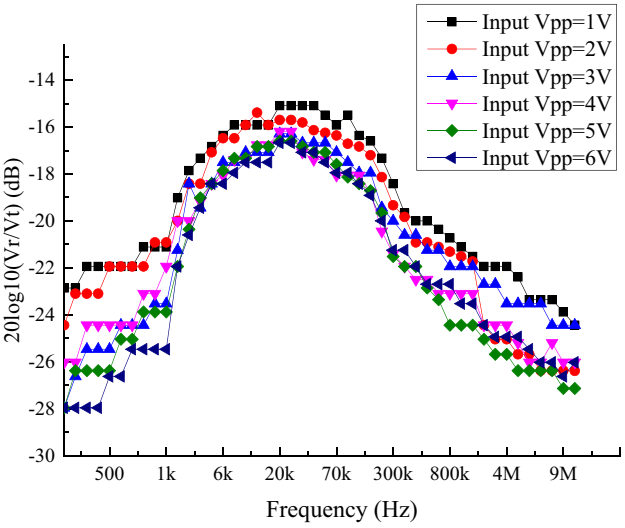

Figure 9. Gain of signal channel corresponding to length 5 cm.

In addition, it must be noticed that the gain of the received voltage varies very slightly with the transmitted voltage in the simulation model. To some extent, the gain does not vary if the frequency does not change. It is also found that the equivalent impedance of electrode R1, R2, R3, R4 and capacitors C1, C2, C3, C4 mainly affect the amplitude rather than the gain of received voltage. As mentioned above, the gain is primarily affected by parasitic capacitances of electrodes. Therefore, the effect of equivalent parasitic capacitances C5, C6, C7, C8 with different values is simulated as well. The results show that the equivalent C6, C8 between transmitted electrode and received electrode primarily affect the signal gain. The equivalent C5 between transmitted electrodes and C7 between received electrodes primarily affect the bandwidth of transmission.

5. CONCLUSION

In this paper, a circuit-coupled FEM model considering the effect of parasitic capacitances between electrodes has been presented for the galvanic coupling IBC with the frequency range from 100 Hz to 10 MHz. Based on the model, the distribution of current density and electric field, the electric potential difference between received electrodes and the signal gain have been focused on. We find that the parasitic capacitances between electrodes are the main factors of signal attenuation with frequency, and it would also affect the amplitude, bandwidth, and cut-off frequency of received signal. To validate the accuracy of the model, an IBC experiment on human arm has been carried out, and the results demonstrate that the proposed model meets the actual situation of IBC much better than the traditional FEM or circuit model. It also reveals that the parasitic capacitances cannot be ignored and must be considered in IBC modeling. In the next work, we will focus on extending the model to other parts of human body and the possible application of these findings to the design of wireless medical healthcare devices.

ACKNOWLEDGMENT

This work was supported by the Natural Science Foundation of Fujian Province of China under grant 2018J01565, the Scientific Research Climbing Plan of Xiamen University of Technology under grant XPDKQ18021, and the Project for Advanced Scientists of Xiamen University of Technology under grant YKJ19016R.

REFERENCES

1. Zimmerman, T. G., "Personal area networks: Near-field intra-body communication," M.S. thesis, MIT Media Lab., Cambridge, MA, Sep. 1995.
2. Kobayashi, T., Y. Shimatani, and M. Kyoso, "Application of near-field intra-body communication and spread spectrum technique to vital-sign monitor," *Engineering in Medicine and Biology Society (EMBC), 2012 Annual International Conference of the IEEE*, 4517–4520, 2012.
3. IEEE Standard for Local and Metropolitan Area Networks — Part 15.6: Wireless Body Area Networks, IEEE Standard 02.15.6-2012, 1–271, 2012.
4. Seyedi, M., B. Kibret, D. T. H. Lai, and M. Faulkner, "A survey on intrabody communications for body area network applications," *IEEE Transactions on Biomedical Engineering*, Vol. 60, No. 8, 2067–2079, 2013.
5. Lucev, Z., I. Krois, and M. Cifrek, "A capacitive intrabody communication channel from 100 kHz to 100 MHz," *IEEE Transactions on Instrumentation and Measurement*, Vol. 61, No. 12, 3280–3289, 2012.
6. Xu, R., H. Zhu, and J. Yuan, "Electric-field intrabody communication channel modeling with finite-element method," *IEEE Transactions on Biomedical Engineering*, Vol. 58, No. 3, 705–712, Mar. 2011.
7. Callejon, M. A., J. Reina-Tosina, D. Naranjo-Hernandez, and L. M. Roa, "Galvanic coupling transmission in intrabody communication: A finite element approach," *IEEE Transactions on Biomedical Engineering*, Vol. 61, No. 3, 775–783, 2014.
8. Pun, S. H., Y. M. Gao, P. U. Mak, M. I. Vai, and M. Du, "Quasi-static modeling of human limb for intra-body communications with experiments," *IEEE Trans. Inf. Technol. Biomed.*, Vol. 15, No. 6, 870–876, Nov. 2011.
9. Hachisuka, K., Y. Terauchi, Y. Kishi, et al., "Simplified circuit modeling and fabrication of intrabody communication devices," *Sens. Actuators A*, Vols. 130–131, 322–330, Jun. 2006.
10. Haga, N., K. Saito, M. Takahashi, et al., "Equivalent circuit of intrabody communication channels inducing conduction currents inside the human body," *IEEE Transactions on Antennas and Propagation*, Vol. 61, No. 5, 2807–2816, 2013.
11. Kibret, B., M. Seyedi, D. T. Lai, et al., "Investigation of galvanic-coupled intrabody communication using the human body circuit model," *IEEE J. Biomed. Health Inform.*, Vol. 18, No. 4, 1196–206, Jul. 2014.
12. Swaminathan, M., F. S. Cabrera, J. S. Pujol, U. Muncuk, G. Schirner, and K. R. Chowdhury, "Multi-path model and sensitivity analysis for galvanic coupled intra-body communication through layered tissue," *IEEE Transactions on Biomedical Circuits and Systems*, Vol. 10, No. 2, 339–351, Apr. 2016.
13. Callejón, M. A., D. Naranjo-Hernandez, J. Reina-Tosina, and L. M. Roa, "Distributed circuit modeling of galvanic and capacitive coupling for intrabody communication," *IEEE Transactions on Biomedical Engineering*, Vol. 59, No. 11, 3263–3269, Nov. 2012.
14. Xu, R., H. Zhu, and J. Yuan, "Circuit-coupled FEM analysis of the electric field type intra-body communication channel," *Proc. IEEE Biomed. Circuits Syst. Conf.*, 221–224, Nov. 2009.
15. Gao, Y. M., Z. M. Wu, S. H. Pun, et al., "A novel field-circuit FEM modeling and channel gain estimation for galvanic coupling real IBC measurements," *Sensors (Basel)*, Vol. 16, No. 4, Apr. 2, 2016.

16. Gabriel, S., R. W. Lau, and C. Gabriel, "The dielectric properties of biological tissues: III. Parametric models for the dielectric spectrum of tissues," *Phys. Med. Biol.*, Vol. 41, No. 11, 2271–2293, 1996.
17. Gao, Y. M., "Investigation of electromagnetic model and empirical analysis for galvanic coupling intra-body communication," Ph.D Thesis of Fuzhou University, 103–105, 2010.
18. Cho, N., J. Yoo, S.-J. Song, et al., "The human body characteristics as a signal transmission medium for intrabody communication," *IEEE Transactions on Microwave Theory and Techniques*, Vol. 55, No. 5, 1080–1086, 2007.
19. Chen, Z. Y., Y. M. Gao, and M. Du, "Multilayer distributed circuit modeling for galvanic coupling intrabody communication," *Journal of Sensors*, Vol. 2018, 8096064, 2018.